ISSN 2348 - 0319

Journal home page: http://www.journalijiar.com

INTERNATIONAL JOURNAL OF INNOVATIVE AND APPLIED RESEARCH

RESEARCH ARTICLE

NO_2gas sensing property of nanocrystalline tungsten oxide thick film sensor

***Nisha R.[1], K. N. Madhusoodanan[1] and V. S. Prasad[2]**

1. Dept. of Instrumentation, Cochin University of Science and Technology, Cochin 682022, India.
2. Functional Materials, Material Science and Technology Division, National Institute for Interdisciplinary Science and Technology, Thiruvananthapuram 695019, India.

Abstract:

Nanocrystalline thick film sensors are prepared and investigated for sensitive detection of NO_2 gas. Temperature dependent NO_2gas sensing characteristics are investigated over a temperature range of 100-225^{0}C in air. Optimum operating temperature for NO_2 sensing is found to be 200^{0}C. Sensor response is investigated for various concentrations and the lowest measurable concentration is found to be 1.8 ppm. It is found that tungsten oxide based thick film sensor is a good candidate for NO_2 sensors with satisfactory response and recovery times at optimum temperature of 200^{0}C. The detection mechanism associated with NO_2gas sensing is also discussed. The prepared sensor is characterized by XRD, SEM, TEM, Raman spectroscopy and XPS.

Key Words: Tungsten oxide sensor, thick film, NO_2gas sensing, nanocrystalline, metal oxide sensor

1.Introduction

In recent years, air pollution has been becoming more and more serious with the development of industry and the increase of people life. Nitrogen oxides, NO and NO_2, generated from combustion facilities and automobiles are air pollutants which give damages to human respiratory organs and nerves or cause acid rain, as now recognized worldwide. Compact solid state sensors for detecting NO_X in combustion exhausts and environments are eagerly demanded for the sake of combustion- exhaust control and environmental monitoring. Hence commercially inexpensive, small size and maintenance free solid state sensors for monitoring these gases are urgently needed.

Many metal oxide semiconductors have been utilized as gas sensing active materials for half a century[1]. Among them ZnO, WO_3, and SnO_2 have widely been studied .The gas sensing properties of these materials are related to the surface states and morphology of the material. The operation of most of the metal oxide semiconductor gassensors is based on a reversible change of conductivity due to the adsorption of the gases. The adsorption of gases basically occurs at the surface level of a sensing film, and an increase in the active surface area of the semiconductor oxide would enhance the properties of the materials used for gas sensors. The mechanism of the electrical conductivity change of the oxide under gas exposure is understood in terms of adsorption –desorption reactions involving surface oxygen vacancies. One of the promising solid state metal oxide semiconductor chemosensor is a tungsten oxide based gas sensor. Tungsten oxide (WO_3) is an n-type semiconductor with a reported band gap of about 2.6-2.8eV [2].The intrinsic conductivity arises from its non-stoichiometric composition giving rise to a donor level formed by oxygen vacancy defect in the lattice. Tungsten has many oxidation states i.e 2,3,4,5 and 6.The typical forms of tungsten oxides are tungsten(VI) oxide (WO_3, lemon yellow appearance) and tungsten(IV) oxide (WO_2, brown and blue appearance).Such electronic properties make the tungsten oxides suitable for various applications such as electrochromic [3], photochromic [4], photocatalyst [5]. WO_3 films are reported to have promising electrical properties for gas sensing applications. Several studies have proved that this sensor could be used for the detection of NO_2[6-14] , NO[6,15-19] ,ammonia vapors[10,16,19,20-23], hydrogen sulphide[24-28], CO[29,30] and hydrocarbons[23,29].These films are particularly attractive because they show a high catalytic behaviour both in oxidation and reduction reactions on their surface.

Nanocrystalline materials are in the focus of contemporary materials research as a consequence of the superior properties that are achievable when materials are built up from structural units with sizes on the nanometer scale. There has been an increasing interest in the study of nanocrystalline materials owing to their electrical, optical, mechanical and magnetic properties being superior to those of conventional coarse- grained structures. Gas sensing applications of nanocrystalline materials have received considerable interest in recent years. The surface- to-bulk ratio for a nanocrystalline material is much greater than for a material with large grains, which yields a large interface between the solid and a gaseous or liquid medium. The interaction between a gas and a solid mainly takes place on the surface and hence the amount of atoms residing at grain surfaces and interfaces is critical for controlling the properties of the gas sensor. It has been shown that nanocystalline WO_3 films exhibit very interesting sensor properties and are candidates for detecting toxic gases such as H_2S[27] , NO_2[9] ,CO[30].

In this context we have investigated the sensing characteristics of WO_3 nanoparticles to NO_2 gas in the 1.8 to 86 ppm range at working temperatures of the range of 100 to 225^{0}C.Semiconductor gas sensors based on nanocrystalline WO_3 powders were prepared by acid precipitation method. The thick films of the powder were coated on to glass substrate, annealed at 600^{0}C and its response to different concentration of NO_2 gas was studied. Sensor behavior is presented in detail for representative concentration of 7 ppm. Our study shows that WO_3 nanoparticles are good candidates for sensing NO_2 at a temperature of 200^{0}C.

2. Experimental

2.1. Sensor Fabrication

The WO_3 nanoparticles were synthesized by precipitation technique from aqueous solutions of ammonium tungstate parapentahydrate [31]($(NH_4)_{10}W_{12}O_{41}.5H_2O$, Wako) and nitric acid (HNO_3, Merck). A predetermined amount of tungstate salt was dissolved in de-ionized water and resulting solution was brought to 80^{0}C. With vigorous stirring, a warm, concentrated nitric acid was added drop wise. With continuous stirring the mixed solution was kept at 80^{0}C for 30minutes.The precipitates were allowed to settle for 1 day at room temperature. Precipitate was washed by addition of a large amount of de-ionized water into precipitate followed by stirring for about 10 minutes and allowing precipitates to settle down before decanting the liquid. This washing procedure was carried out six to seven times. The precipitates were dried at 100^{0}C overnight and then calcined in air at a temperature of 400^{0}C for 6hrs.The calcined precipitate was finely powdered in a mortar. For sensor preparation the powder were dispersed in methanol and painted on to a glass substrate .Thus a thick film of the sensor material was obtained. The sensor was then annealed at a temperature of 600^{0}C overnight prior to the temperature dependent measurements.

2.2. Gas sensing set up

The gas sensing measurements of the thick film sensor were tested on indigenously developed static gas characterization system. The details of the test system are reported elsewhere [32]. The test system consisted of a stainless steel chamber of diameter 7.5cm and 6.35cm height. Effective volume of the chamber was 280ml. An inlet was provided for inserting desired concentration of gas to the chamber. An outlet is also provided to remove the gas. The precalibrated gas cylinders were obtained from laboratories. The gas was injected into test chamber with a syringe through an inlet provided with septum. Electrical connections from the sensor were made using two thin copper wires, bonded to the sensor with silver paint. The sensing capability of the sensor was characterized at different operating temperatures to find out optimum working temperature. A heater is incorporated in the chamber in order to heat sample to desired temperature. A resistance temperature detector (RTD) is used to sense temperature. Feed throughs are provided on the top of the chamber for electrical connections to the heater as well as for the temperature sensor (RTD). A microcontroller based PID temperature controller was used to control the operating temperature of the sensor to an accuracy of 0.5°C. Electrical characterization of the WO_3 thick films in presence of the gas were obtained by measuring the change in resistance of films. A keithley 195A digital multimeter is used to measure the resistance of the sensor which is interfaced to the system by a GPIB interface. The programming for the interface is done using BASIC language.

2.3. Characterization

The crystalline structure and particle size of the as prepared powder sample and 600^{0}C annealed thick film sensor were examined by X-ray diffraction measurement (XRD, Bruker AXS D8 Advance). The crystallite size (D) was calculated from peak broadening using the Scherrer approximation, which is defined as

$$D = \frac{0.9\lambda}{B\cos\theta} \quad (1)$$

Where λ is the wavelength of the X-ray (1.5418 A^0), B is the full width at half maximum (FWHM, radian) and θ is the Bragg angle (degree).Raman spectra of 600^0C annealed WO_3 thick film sensor was obtained using Horiba JobinYvonLabRam HR system at a spatial resolution of 2 mm in a backscattering configuration. The 514.5 nm line of Argon ion laser was used for excitation. Surface morphology and compositional analysis of thick films were examined using scanning electron microscopy (SEM, JEOL Model JSM - 6390LV) .TEM (FEI, TECNAI 30G2 S-TWIN microscope) image of 600^0C overnight annealed sensor powder was also obtained. The electronic structure of the surface of WO_3 was performed by X-ray photoelectron spectroscopy (XPS) with a SPECS GmbH spectrometer (Phoibos 100 MCD Energy Analyzer) using MgKα radiation (1253.6 eV).

3. Results and Discussion

3.1. Structural characterization

Figure 1 shows the XRD spectra of as prepared precipitate calcined in air at a temperature of 400^0C for 6hr and thick film sensor of WO_3 annealed at 600^0C overnight. Main peaks were found at $2\theta = 23.0^0$, 23.6^0 and 24.3^0, which were identified as corresponding to Miller index (002), (020), and (200), respectively, in triclinic WO_3 (JCPDS# 20-1323). Hence the 600^0C overnight annealed powder was identified by XRD as nanocrystalline WO_3 .Using Scherrer equation average crystallite size of the WO_3 thick film sensor were found to be 30nm.

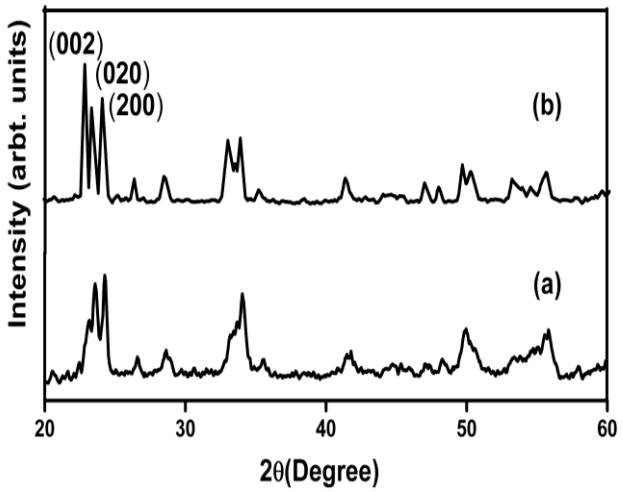

Figure1. XRD patterns (a) WO_3 precipitate calcined at 400^oC for 6 hr (b) thick film sensor annealed at 600^0C overnight

Raman spectrum of 600^0C annealed tungsten oxide thick film sensor is shown in figure 2. The spectrum can be divided into three main regions at 900-600, 400-200 and below $200cm^{-1}$. Peaks below $200cm^{-1}$ are associated with lattice modes, the intermediate frequencies (200–400 cm^{-1}) showing O–W–O bending mode features, and the last at higher frequencies (600–900 cm^{-1}) with the peaks related to W–O stretching modes [33].

Typical surface morphology of thick film sensor annealed at 600^0C overnight is shown in figure 3. It is evident that the material consists primarily of crystalline aggregates and is highly porous in nature. The most important factors that influence the sensor characteristics are probably microstructure and surface area. The films exhibiting a porous structure have a large fraction of atoms residing at surfaces and interfaces between the pores, which suggests that the microstructure of the films is suitable for gas-sensing purposes. In the other words, it can be said that the high sensitivity of a sensor can be attributed to the full exposure of surface adsorption sites to chemical environments. From the SEM images it's clear that our thick film surfaces are highly porous which makes it highly

suitable for sensing application. The particles are found to be spherical in nature. The energy dispersive X-ray analysis, which is shown in the inset, reveals that only oxygen and tungsten elements are present.

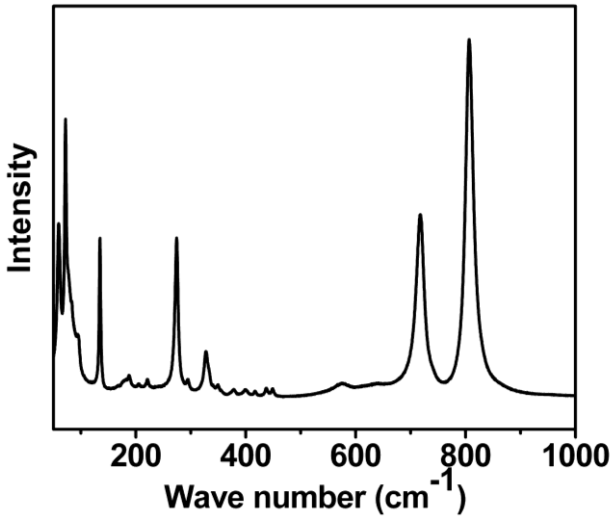

Figure 2. Raman spectra of 600^0C annealed tungsten oxide thick film sensor.

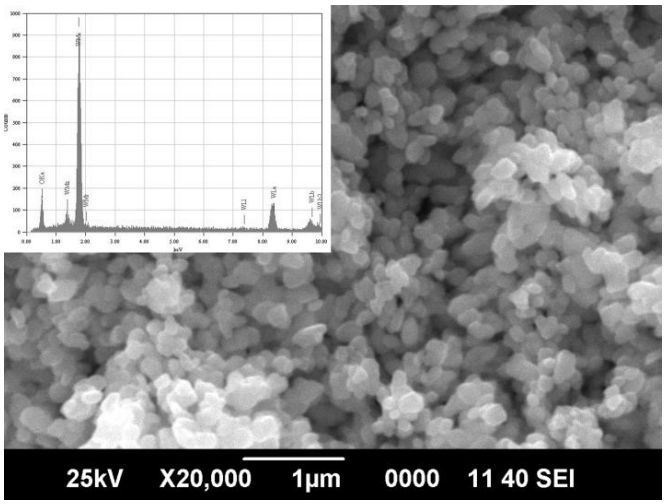

Figure 3. SEM image of the WO_3 thick film sensor annealed at 600^0C with inset showing EDS spectrum.

Figure 4 show TEM image of the 600^0C annealed thick film sensor WO_3 powder. TEM image also confirms that sensor consists of crystalline aggregates and nanoparticle prepared is spherical in nature as obtained from the SEM results. TEM results support particle size obtained by XRD characterization.

In order to understand the chemical composition of tungsten oxide film, we carried out XPS measurement. XPS spectrum of the 600^0C annealed sample is illustrated in figure 5. The W 4f core level spectrum recorded on 600^0C annealed samples shows the two components associated with W $4f_{5/2}$ and W $4f_{7/2}$ spin orbit doublet at 36.8 and 34.9 eV. Binding energy values obtained for the spin orbits shows a small shift towards the lower binding energy. This shift may be caused by the contribution from W^{5+} or W^{4+} states, resulting in oxygen vacancies in thick film sensor[34]. The O1s peak is located at 529.7 eV, which is ascribed to the W-O peak.

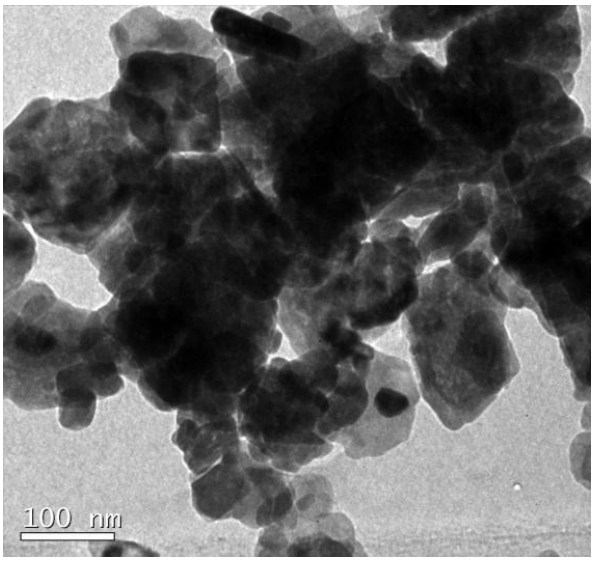

Figure 4.TEM image of the WO_3 thick film sensor annealed at 600^0C.

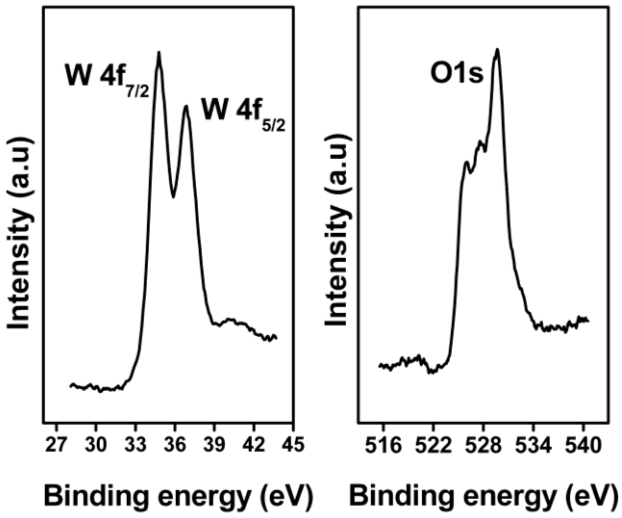

Figure 5. XPS spectrum of the 600^0C annealed sensor

3.2. NO_2 gas response studies

Gas sensing capability of thick film sensors were measured to oxidising gas NO_2 in air at a temperature range 100 to 225^0 C. Initial gas sensing experiments were performed at room temperature to measure the response of WO_3 films to test gas. However, as almost no response was observed for measurements at room temperature. Hence electrical conductance measurements were performed at various temperatures in order to determine the temperature at which the WO_3 sensors are most sensitive to analyzed gas. The temperature at which sensors are most sensitive to analyzed gases is defined as optimum working temperature of the sensor. In general, it is known that the sensitivity of the sensors is affected by the working temperature. The higher temperature enhances surface reaction of sensors and gives higher sensitivity in that temperature range. The interaction between metal oxide and adsorbed gas is a dynamic process. When the film is exposed to a test gas in air, the adsorption and desorption processes occur simultaneously. In the response process the adsorption dominates on desorption process until stationary conditions are attained. In this situation the number of adsorbed gas molecules will be equal to the number of the desorbed

ones, and the electrical conductivity attains a constant value. After the test gas is cut off, the desorption prevails on the re-adsorption process and the conductivity will return to its original value.

Samples were exposed to variable concentrations in the range 1.8 to 86 ppm. Since WO_3 is an n type semiconductor resistance increases on exposure to oxidising gas like NO_2. Sensor sensitivity is defined as $S=R_{gas}/R_{air}$, where $R_{gas}$is resistance of sensor in presence of gas and R_{air} is resistance of sensor before introduction of gas. Response time is defined as time required for resistance to reach 90% of equilibrium value after test gas is injected. Recovery time is time necessary for sensor to attain a resistance of 10% of original value in air. Gas sensing characteristics of thick film sensor to a concentration of 7 ppm studied is discussed in detail. Similar results were obtained for higher concentrations studied. Sensitivity of sensor at different operating temperature to a concentration of 7 ppm is shown in figure 6. Response and recovery time sensor characteristics to 7 ppm concentration studied is illustrated in figure 7 (a) and (b) respectively.

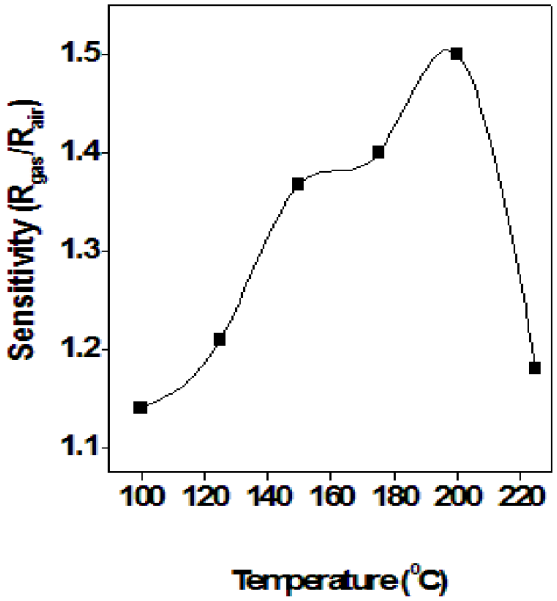

Figure 6. Sensitivity of sensor at different operating temperature to a concentration of 7 ppm NO_2 gas

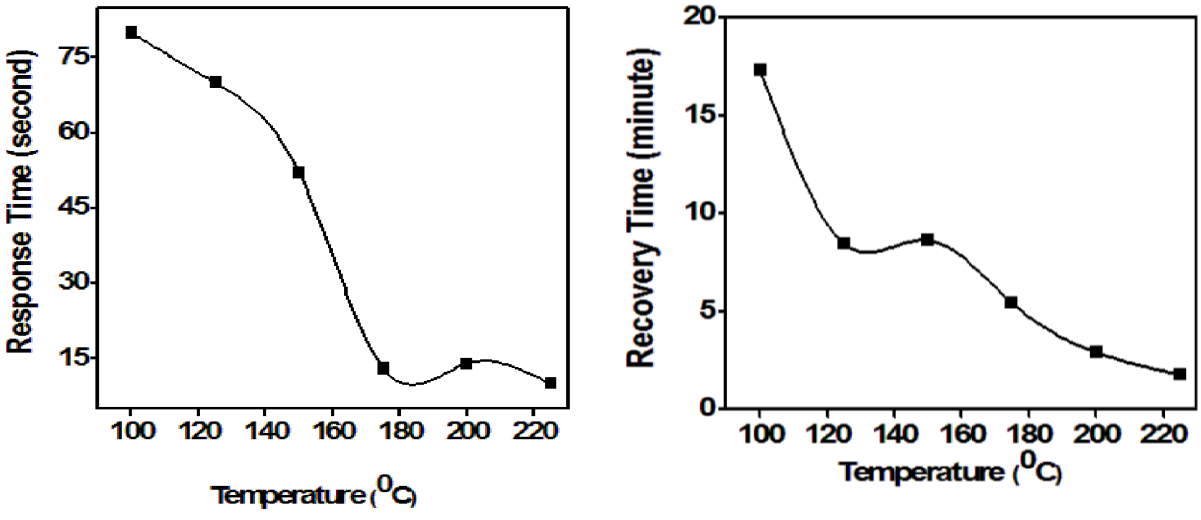

(a) (b)

Figure 7 (a) Response time (b) Recovery time of sensor to 7 ppm of NO_2 gas at temperatures ranging from 100^0C to 225^0C

Temperature dependent gas sensing investigation proves that at a temperature of 200^0C the sensitivity is maximum. Beyond this temperature the sensitivity of sensor decreases.Selecting optimum temperature is a critical factor in the operation of gas sensors. Considering sensitivity, response time and recovery time at different temperatures, 200^0C was considered as optimum operating temperature for the working of WO_3 sensor. At this temperature a maximum sensitivity of 1.5 was achieved for 7 ppm NO_2 with lower response and recovery time. At 200^0C response time and recovery time were relatively small and has a value of 14 seconds and 2.9 minutes respectively. Hence further studies depending on various concentrations were carried out at this optimum temperature of 200^0C. Sensitivity of sensor to different concentration ranging from 1.8 to 86 ppm were studied at optimum temperature of 200^0C is illustrated in figure 8. The concentration dependent gas sensing behaviour shows that for a concentration of 86 ppm the sensitivity is as high as 58. These results prove that the sensors are highly sensitive at higher concentration. Response of sensor to different concentrations at optimum operating temperature of 200^0C is shown in fig. 9 (a) and (b).

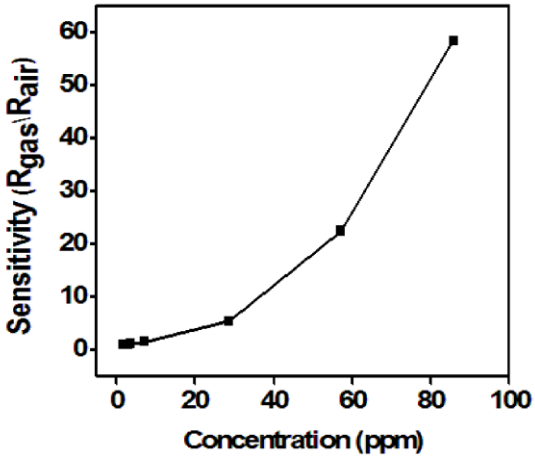

Figure. 8 Sensitivity of WO_3 thick film sensor towards different concentrations of NO_2 gas at 200^0C

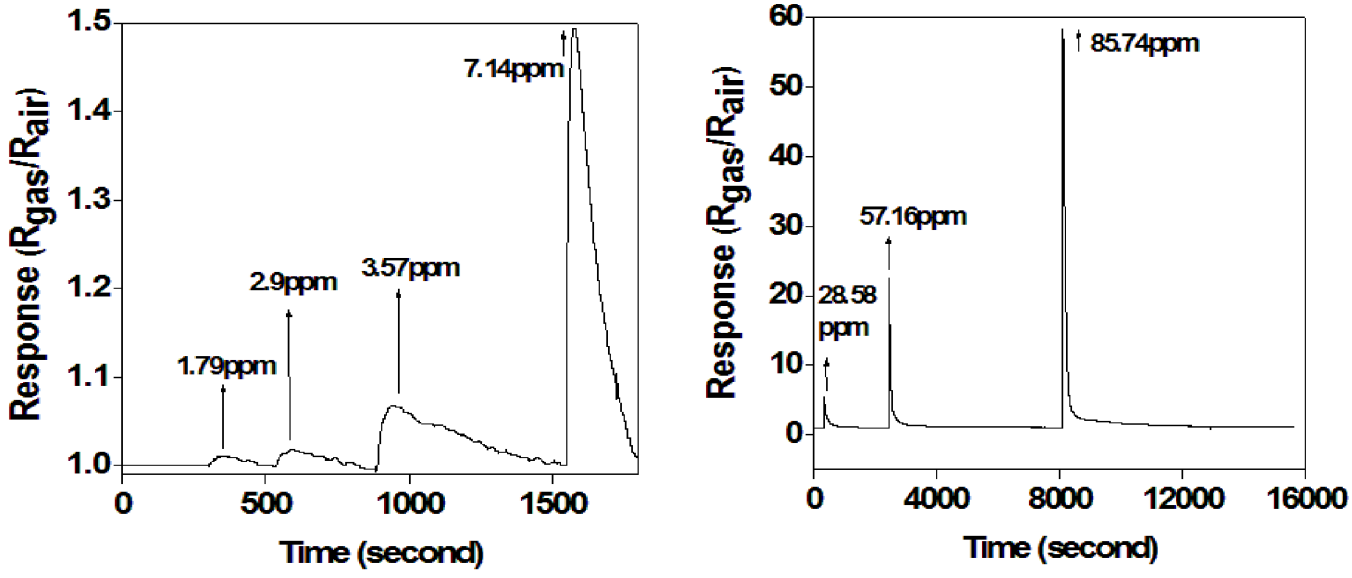

(a) (b)

Fig. 9 (a) and (b) Response of WO_3 thick film sensor towards different concentrations of NO_2 at 200^0C

It is known that sensing mechanism of oxide materials is surface controlled in which grain size, surface states and oxygen adsorption play an important role[35]. The larger surface area generally provides more adsorption–desorption sites and thus higher sensitivity. The sensor element consists of semiconductor nanoparticle. The microstructure and morphology of these aggregates are considered to be very important for the transducer function. Each particle is connected with its neighbors either by grain-boundary contacts or by necks. In the case of grain-boundary contacts, electrons should move across the surface potential barrier at each boundary. The change of the barrier height makes the electric resistance of the element dependent on the gaseous atmosphere, as first pointed out by Ihokura [36]. The resistance, and hence the gas sensitivity, in this case are not basically dependent on the particle size. In the case of necks, electron transfer between particles takes place through a channel which is formed inside the space-charge layer at each neck. The width of the channel is determined by the neck size and thickness of the surface charge layer (L)and its change with gases gives rise to the gas-dependent resistance of the element, as first pointed out by Mitsudo[37]. Obviously the gas sensitivity in this case is dependent on the particle size. These two models, although rather conceptual, indicate the importance of the microstructure for the transducer function of the element. Tamaki et al. [7] studied the grain size effects in WO_3 for nitrogen oxide detection. The results indicate that for a crystallite size greater than 30nm the conduction is under grain boundary control. The average crystallite size of WO_3 sensor is 30nm. Hence we deduce that in our sensors the conduction is through grain boundary contacts.

Studies on operation mechanism of semiconductor gas sensors indicate that most target gases are detected due to influence of adsorbed oxygen. Atmospheric oxygen gets adsorbed on surface of metal oxide removing electrons from conduction band of sensing metal oxide and occurs on surface in form of O^-, O^{2-} and O_2^- creating a thin layer of depletion region at the surfaces of WO_3 grains[38]. The reaction is as follows where (gas) denotes gaseous phase and (ads) denote adsorbed species respectively.

$$O_2\,(gas) \leftrightarrow O_2\,(ads) \quad (2)$$

$$O_2\,(ads) + e^- \leftrightarrow O_2^-\,(ads) \quad (3)$$

$$O_2^-\,(ads) + e^- \leftrightarrow 2O^-\,(ads) \quad (4)$$

$$O^-\,(ads) + e^- \leftrightarrow O^{2-}\,(ads) \quad (5)$$

Reaction (3) usually occurs at temperature below 175^0C and reactions (4) and (5) occur at temperature above 175^0C.

When WO_3 based sensor material is exposed to atmosphere of NO_2, resistance of the sensor increases. The potential theory suggested that a potential barrier is formed between the surface of semiconductor film and the ambient environment [39]. NO_2 gets adsorbed onto WO_3 surface, and the oxygen of NO_2 served as the accepter, extracting electrons from the conduction band of WO_3. Therefore, the barrier of $WO_3$is increased and resistance of the WO_3film also increases whenever $NO_2$is adsorbed on WO_3 surface. NO_2 can not only capture the electrons of the semiconductor due to its higher electrophilic property, but also react with the adsorbed oxygen ion leading to the formation of adsorbed NO_2^-, the process of the reaction can be described as follows [40].

$$NO_{2(g)} + e^- \rightarrow NO_{2\,(ads)}^- \quad (3.6)$$

$$NO_{2(g)} + O_{2\,(ads)}^- + 2e^- \rightarrow NO_{2\,(ads)}^- + 2O_{(ads)}^- \quad (3.7)$$

The above reactions decreased the concentration of electron on the surface of material, thus resulting in an increase of the material resistance. In addition, the reaction occurs between $NO_{2\,(ads)}^-$ and $O_{2\,(ads)}^-$:

$$NO_{2\,(ads)}^- + O_{2\,(ads)}^- \rightarrow 2O_{(ads)}^- + NO_2 \quad (3.8)$$

Thus the cyclic reaction continues. These series of reactions resulted in the concentration of electron on the surface of the material to further decrease, which led to the decrease in conductivity of the material (increase of the resistance) and hence the detection of NO_2 is achieved.

The temperature dependent NO_2 gas sensing results (fig. 6) indicate that the sensitivity of WO_3 sensor increases with increasing temperature up to the optimum operating temperature. A further increase of the

temperature reduces the response value. At lower temperature a low interaction happens between adsorbed oxygen species and detected NO_2 gas. Thus the response of the WO_3 thick film sensor is low at lower temperature. At higher temperature some of the adsorbed oxygen species may be desorbed from the film which contributes to low response value. When the operating temperature is very high the charge carrier concentration is also very high in a semiconductor. The electrons received by adsorbed NO_2 gas is much less than the number of charge carriers in sensitive material, which hardly causes the conductivity change of the sensitive film. As a result, there is an optimal operating temperature to balance the above two effects in order to achieve maximum gas response. In WO_3 based sensors the optimal operating temperature was found to be 200^0C beyond which the sensitivity of the sensor decreases.

Semiconductor sensors sensed gas using its non-stoichiometric structure and the free electrons originated from the oxygen vacancy. The sensing properties of WO_3 were controlled by the surface defect and structure rather than the native properties according to Bringans et al. [41]. There is more oxygen vacancies on the surface of WO_3calcined at higher temperature [42]. The amount of chemisorbed oxygen on surface and surface species available for adsorption highly influences the change in conductivity [43]. In WO_3 the chemisorptions sites are owing to the various oxidation states of tungsten arising because of the oxygen deficiency created atthe annealing temperature. The XPS studies on WO_3 also reveal that there is a shift in oxidation state of tungsten from +6, the oxidation state of tungsten in stoichiometric WO_3. This shift may be caused by the contribution from W^{5+} or W^{4+} states, resulting in oxygen vacancies in thick film sensor. Accordingly, a possible interaction mechanism between nitrogen dioxide and WO_3 may be as follows.

$$NO_2 + W^{5+} \leftrightarrow W^{6+} + NO_2^- \qquad (3.9)$$

It has been reported earlier that when annealing temperature increases over 400^0C [44], reactive sites for the adsorption of NO_2 and oxygen molecules are created owing to the drifting of oxygen deficiencies to surface [40,45]. The presence of unsaturated bonds on the material surface may lead to the formation of chemical bonds between gaseous species and metal oxides. Hence the amount of chemisorbed species increases with surface defect concentration [46] thereby increasing the sensitivity of WO_3 film to NO_2 gas.

4. Conclusion

Thick film sensor of tungsten oxide was prepared by dispersing the prepared tungsten oxide powder in methanol and drop casting on glass substrates followed by overnight annealing at 600^0C. The obtained crystalline phase of WO_3 nanoparticles was triclinic in nature. The crystalline structure of sensor was characterized using XRD. The surface morphology and elemental composition were characterized by scanning electron microscopy and energy dispersive X-ray analysis. SEM investigationsobserved that WO_3 samples consisted of crystalline aggregates. This was confirmed in TEM results. SEM and TEM investigations on the 600^0C annealed sensor proved that the sensor consisted of nanoparticle particles which were spherical in nature.Temperature dependent gas sensing properties of samples were studied for the detection of NO_2gas. Resistance of the films increases upon exposure to gases and attained a saturation value. Sensor regains its original value after test gas is removed. Sensor exhibit good sensing characteristics to NO_2 in the concentration range studied, 1.8 to 86 ppm over the temperature range 100-225^0C. The best results were obtained at operating temperature of 200^0C with a sensitivity of 1.5 for 7 ppm concentration. Response and recovery time of sensor at this optimum temperature was 14 seconds and 2.9 minutes respectively for 7 ppm concentration. Lowest measurable concentration is found to be 1.8 ppm. Resistance always returned to its initial value after the test gas is shut off for all concentration studied. Results indicate that response of sensor is reproducible during this test. The sensing mechanism associated with NO_2 sensing is also discussed.

Acknowledgements

The authors wish to acknowledge Dr.M.K.Jayaraj, Nanophotonic& Optoelectronic Devices laboratory, Dept. of physics for Raman measurements under DST nano mission initiative programme and Dr. Prof. G. Mohan Rao, Department of Instrumentation and Applied Physics, Indian Institute of Science, Bangalore for XPS measurement. We are thankful to SAIF, Cochin University of Science and Technology, Kochi, Kerala, India for the XRD and SEM measurements.

References

1. G.Eranna, B.C. Joshi, D.P. Runthala , R.P.Gupta , Oxide materials for Development of Integrated Gas Sensors – A comprehensive Review, Crtical Reviews in Solid State and Materials Sciences 29 (2004)111-188.

2. M. A. Butler Photo electrolysis and physical properties of the semiconducting electrode WO_2,J.Appl.Phys. 48 (1977) 1914- 1920

3. C.G.Ganqvist, Electrochromic tungsten oxide films: Review of progress 1993–1998, Solar Ener.Mater.Solar Cell 60 (2000) 201-262.

4. M.Sun, N.Xu, Y.W.YaoE.G.Wang, Nanocrystalline tungsten oxide thin film: Preparation, microstructure, and photochromic behavior,J.Mater.Res. 15 (2000) 927-933.

5. G.R.Bamwenda, H.Arakawa, The visible light induced photocatalytic activity of tungsten trioxide powders ,Appl.Catal.A 210 (2001) 181-191.

6. M.Akiyama, J.Tamaki, N.Miura, N.Yamazoe, Tungsten oxide based semiconductor Sensor Highly sensitive to NO and NO_2, Chemistry Letters 20 (1991) 1611-1614.

7. J.Tamaki, Z.Zhang, K.Fujimori, M.Akiyama, T.Harada, N.Miura, N.Yamozoe Grain size effects in Tungsten oxide based sensor for Nitrogen oxides, Journal of Eletrochemical Society 141 (1994) 2207-2210.

8. D.S. Lee, S.D.Han, J.S.Huh, D.D.Lee, Nitrogen oxides sensing characteristics of WO_3 based nanocrystalline thick film gas sensor, Sensors and Actuators B 60 (1999) 57-63.

9. S.H. Wang , T. C.Chou, C.C. Liu, Nanocrystalline tungsten oxide NO_2 sensor , Sensors and Actuators B 94 (2003) 343-351.

10. T.Siciliano, A.Tepore, G.Micocci, A.Serra, D.Manno, E.Filippo, WO3 gas sensors prepared by thermal oxidization of tungsten Sensors and Actuators B 133 (2008) 321-326.

11. J.Brunet, V.P. Garcia, A.Pauly, C.Varenne, B. Lauron , An optimized gas sensor microsystem for accurate and real- time measurement of nitrogen dioxide at ppb level, Sensors and Actuators B 134 (2008) 632-639.

12. Z.Liua, M. Miyauchi , T. Yamazaki, Y. Shen ,Facile synthesis and NO2 gas sensing of tungsten oxide nanorods assembled microspheres Sensors and Actuators B 140 (2009) 514 -519 .

13. Y. Qin, M. Hu, J. Zhang , Microstructure characterization and NO2-sensing properties of tungsten oxide nanostructures ,Sensors and Actuators B 150 (2010) 339-345.

14. C. Zhang, M. Debliquy, A. Boudiba, H Liao, C. Coddet Sensing properties of atmospheric plasma-sprayed WO_3 coating for sub-ppm NO_2 detection Sensors and Actuators B144 (2010) 280-288.

15. M.Penza, M.A.Tagliente, L.Mirenghi, C.Geradi, C.Martucci, G.Cassano , Tungsten trioxide (WO_3) sputtered thin films for a NO_X gas sensor, Sensors and Actuators B 50 (1998) 9-18.

16. A.A Tomchenko V.V. Khatko, I.L. Emelianov , WO3 thick-film gas sensors, Sensors and Actuators B 46 (1998) 8-14.

17. A.A. Tomchenko, I.L. Emelianov, V.V. Khatko ,Tungsten trioxide-based thick-film NO sensor: design and investigation , Sensors and Actuators B 57 (1999) 166-170.

18. X.Wang, N.Miura, N.Yamazoe, Study of WO_3 based sensing materials for NH_3 and NO detection , Sensors and Actuators B 66 (2000) 74-76.

19. T.Siciliano, A.Tepore, G.Micocci, A.Serra, D.Manno, E.Filippo ,WO_3gas sensors prepared by thermal oxidization of tungsten ,Sensors and Actuators B 133 (2008) 321-326.

20. B.T.Marquis, J.F.Vetelino, A semiconducting metal oxide sensor array for the detection of NO_x and NH_3 Sensors and Actuators B 77 (2001) 100-110.

21. M.Stankova, X. Vilanova, E.Llobet, J.Calderer, C.Bittencourt, J.J.Pireaux, X.Correig, Influence of the annealing and operating temperatures on the gas sensing properties of rf sputtered WO_3 thin –film sensors, Sensors and Actuators B 105 (2005) 271-277.

22. Y.S.Kim, S.C.Ha, K.Kim, H.Yang S.Y. Choi , Y.T. Kim J.T.ParkC.H.Lee, J.Paek, K.Lee ,Room temperature semiconductor gas sensor based on nonstoichiometric tungsten oxide nanorod film , Applied Physics Letters 86 (2005) 213105-1 213105-3

23. Y.S.Kim ,Thermal treatment effects on the material and gas sensing properties of room temperature tungsten oxide nanorod sensors, Sensors and Actuators B 137 (2009)297-304.

24. E.P.S.Barrett, G.C Georgiades ,P.A.Sermon , The mechanism of operation of WO_3 based H_2S sensors, Sensors and Actuators B 1 (1990) 116- 120.

25. H.M.Lin, C.M.Hsu, H.Y. Yang, P.Y Lee, C.C. Yang , Nanocrystalline WO_3 based H_2S Sensors, Sensors and Actuators B 22 (1994) 63-68.

26. T.L.Royster Jr., D.Chatterjee, G.R.Paz-Pujalt, C.A.Marrese , Fabrication and evaluation of thin –film solid -state sensors for hydrogen sulphide detection, Sensors and Actuators B 53 (1998) 155-162 .

27. J.L.Solis ,S.Saukko, L.B.Kish, C.G.Granqvist, V.Lantto ,Nanocrystalline tungsten oxide thick films with high sensitivity to H_2S at room temperature ,Sensors and Actuators B 77 (2001) 316-321.

28. C.S.Rout, M.Hegde, C.N.R. Rao H_2S sensors based on tungsten oxide nanostructures, Sensors and Actuators B 128 (2008) 488 - 493.

29. I.Jimenez, J. Arbiol, G.Dezanneau, A.Cornet, J.R.Morante, Structural and Gas Sensing Properties of WO_3 Nanocrystalline powders obtained by a Sol-Gel Method from Tungstic acid, IEEE sensors Journal 2 (2002) 329- 334.

30. T.D. Senguttuvana, VibhaSrivastava, Jai S. Tawal, Monika Mishra, ShubhdaSrivastava, Kiran Jain, Gas sensing properties of nanocrystalline tungsten oxide synthesized by acid precipitation method ,Sensors and Actuators B 150 (2010)384-388.

31. S. Supothina , P. Seeharaj, S. Yoriya and M. Sriyudthsak , Synthesis of tungsten oxide nanoparticles by acid precipitation method Ceramics International 33, (2007), 931-936.

32. Nisha R, Madhusoodanan K N, SreejithKarthikeyan, Arthur E. Hill, and Richard D. Pilkington, NO2 Gas Sensing Properties of In_2O_3Thin Films Prepared by Pulsed D.C MagnetronSputtering Technique , Energy and Environment Focus , 2, 2013, 157-162.

33. A. Baserga ,V. Russo , F.D. Fonzo , A. Bailini, D. Cattaneo, C.S. Casari, A. L. Bassi and C. E. Bottani Nanostructured tungsten oxide with controlled properties: Synthesis and Raman characterization, Thin Solid Films 515, (2007), 6465 -6469.

34. S.C. Moulzolf , S. Ding and R. J. Lad , Stochiometry and microstructure effects on tungsten oxide chemiresistive films Sensors and actuators B 77, (2001) , 375-382.

35. A. Rothschild and Y. Komem , The effect of grain size on the sensitivity of nanocrystalline metal-oxide gas sensors, J. Appl. Phys. 95, (2004) , 6374 -6380.

36. H. Ihokura, SnO based inflammable gas sensors Doctoral Thesis Kyushu University Japan. (1983)

37. H. Mitsudo, Ceramics for gas and humidity sensors gas sensor, Ceramics 15, (1980), 339-345.

38. K.D. Schierbaum, U.Weimar, W. Göpeland R. Kowalkowski, Conductance, work function and catalytic activity of SnO_2-based gas sensors Sensors and Actuators B 3, (1991) 205-2014.

39. J. Ding, T. J. Mc. Avoy, R. E. Cavicch and semancik Sensors and Actuators B (2001) 77, 597.

40. M. Ivanovskaga, A. Gurlo and P. Bogdanov Sensors and Actuators B (2001) 77, 264.

41. R. D. Bringans, H. Hochst and H.R. Shanks Phys. Rev. B (1981) 24, 3481.

42. H. T. Sun, C. Cantalini, L. Lozzi, M. Passacantando, S. Santucci and M. Pelino Thin Solid Films (1996) 287, 258.

43. J. Mizsei Sensors and Actuators B (1995) 23, 173.

44. W. Mickelson, A. Sussman and A. Zett Applied Physics Letters (2012) 100, 173110.

45. S. R. Aliwell, J. F. Halsall, K. F. E. Pratt, J. O. Sullivan, R. L. Jones, R. A. Cox, S. R. Utembe, G. M. Hansford and D. E. Williams Meas. Sci. and Technol. (2001) 12, 684.

46. E. Henrich and P. A. Cox The surface Science of Metal Oxides Cambridge University Press Cambridge (1994), 257.